Bull. Ind. Soc. Earth. Tech., Paper No. 341, Vol. 31, No. 2, June 1994, pp. 91-115

NOISE CANCELLATION IN RECORDS OF DIGITAL ACCELEROGRAPH THROUGH ADAPTIVE FILTER

S. Basu, Ashok Kumar and Brijesh Chandra
Department of Earthquake Engineering,
University of Roorkee, Roorkee 247667, India.

Abstract

Pre event record of a digital accelerograph is modelled as coloured noise and a scheme is developed which uses adaptive filter to remove instrument and the background noise from the record of digital accelerographs. The effectiveness of the proposed scheme is shown by analysing a record of digital accelerograph. In this example it is first shown that the pre event of the record can be modelled as coloured noise. The proposed scheme is then used to remove the noise adaptively from the recorded acceleration. Comparison of Fourier spectra of pre event record, uncorrected and corrected accelerogram show that noise which was pesent in the uncorrected accelerogram has been satisfactorily removed. Although in this work the scheme has been implemented off-line but it can be used as on-line filter in digital accelerographs. This is perhaps one of the ways by which an accelerograph can also perform the function of a micro earthquake recorder.

INTRODUCTION

The provision of pre-event in digital accelerographs is one of the features which has made them more popular than analog accelerographs. Also data recorded from digital accelerographs have substantially smaller noise to signal ratio in the frequency range of recording as compared to analog accelerographs due to the fact that (a) unlike analog instruments such accelerographs have no moving parts; (b) the data are free from human errors assosiated with digitization and (c) sensors of digital accelerographs (usually force balance accelerometers) are more accurate, have a higher natural frequency and larger dynamic range. Due to these reasons it may be assumed that each record of digital accelerographs has unique noise characteristics which can be determined. In this paper a procedure based on adaptive filters is suggested which uses untriggered portion of the pre-event data to determine the noise characteristics of records. The untriggered portion of pre-event data is taken as noise and is modelled as auto regressive process. The transfer function of the noise so determined is used for noise cancellation for the event to obtain the corrected accelerogram. This noise cancellation is done adaptively. The philosophy of such a correction scheme can be derived taking a cue from the use of adaptive filters in modelling and cancellation of noise in various fields

such as electrocardiogram, echo cancellers, adaptive line enhancers, speech synthesis etc (Goodwin and Sin, 1984). However, the problem of correction of records of digital accelerographs is more complex.

TRANSFORMATION AND NOISE IN DIGITAL ACCELEROGRAPHS

Although the noise to signal ratio in the data recorded from digital accelerographs is far less than that in analog accelerographs (Iwan et. al, 1985) yet, noise creeps in the records of digital accelerographs during transformations at various stages of recording. The first transformation takes place in the accelerometer where acceleration is converted into equivalent voltage. Closed form solution in frequency domain for transfer function of FBA is available (Amini and Trifunac, 1983,1985). This transfer function can be used to get the acceleration from the recorded voltage output through deconvolution.

Another transformation takes place at the signal conditioner. Here the the anti-aliasing filter removes high frequencies and the voltage signal is amplified to the required range. Inspite of the fact that anti-aliasing filter is an essential requirement for any digital recording system, most analog filters like Butterworth produce nonlinear phase shift. Whereas these nonlinear phase shifts should not be of much consequence yet earthquake engineers have objections to these (Lee, 1984). One of the methods of removing this nonlinear phase shift is to design a digital filter having the same performance as that of the analog anti-aliasing filter (Kumar,·1993). This means that operation for $H(jw)$ takes place at analog stage and operation for $H(-jw)$ is performed for the recorded digital data to obtain zero phase shift.

In addition to the above transformations, the system continuously records some noise which may be either instrument noise or background noise. It is this noise which has been examined in detail and a procedure is suggested to remove this noise and obtain the corrected accelerogram. Although in some of the strong motion records this noise may not be of much concern but with the large dynamic ranges available today, it becomes important to analyse such noise and to develop an algorithm for its cancellation. The attempt for such noise cancellation should ultimately aim at incorporating these algorithms as part of hardware and software configuration of the digital accelerograph so that such noise cancellation takes place during the recording itself. Clearly this would help in employing such accelerographs record microearthquakes also successfully as the filtering of the background noise is an important requirement there. However, in this part of the work attention is confined to develop an algorithm which can identify the transfer function of noise from the pre-event record and affect noise cancellation in the recorded portion. The feasibility of incorporating the algorithm as part of hardware and software configuration of digital accelerograph (perhaps using DSP chips) is presently left out of consideration. However, while developing this algorithm, this requirement is constantly kept in mind.

ADAPTIVE FILTERS FOR NOISE CANCELLATION

Adaptive filters have been widely used for noise cancellation in various disciplines (Goodwin and Sin, 1984) for which statistical characteristics of the signal are not *a priori* known. These problems can be broadly divided into following two catagories.

1. The records of the observed signal (composed of actual signal corrupted with an additive noise) and of reference noise are available for the entire duration. The additive noise is then estimated from the reference noise and subtracted from the observed signal to estimate the noise free signal.

2. In the second class of problems, the signal and noise lie in different bands and only the corrupted signal is available. The adaptive algorithm then uses the properties of the signal and of the noise that lie in different bands. For example consider the signal to be wideband and noise to be narrowband. Since the noise band is narrow in comparison to the signal, the noise part of the sample will be highly correlated. The corrupted signal is delayed long enough to cause the actual signal components contained in it to be uncorrelated and the delayed corrupted signal is passed through an adaptive filter to linearly predict the noise.

However, in case of digital accelerographs, although a record of signal superimposed with noise is available, the categorization of the frequency contents of actual signal and noise can not be made as discussed above. A reference noise is available only in the pre-event portion of the record. This forces one to first examine how the noise should be modelled. Once this question is resolved, an adaptive filter algorithm can be developed to achieve noise cancellation from the recorded signal.

TIME DOMAIN ANALYSIS OF ADAPTIVE FILTER

Records of digital accelerographs comprise samples of ground acceleration combined with environmental and instrument noise. The recorded data in the solid state memory consists of two parts — the pre-trigger and the post-trigger samples. Let K be the number of samples of pre-trigger part and N be the number of samples of post-trigger part. Most of the first part of K samples are the samples of noise only which are recorded prior to the set trigger level. The following N samples include signal and noise. It has been shown by Kumar (1993) that K samples of $x(n)$ in the records of digital accelerograph can be modelled as auto regressive process. This information can be used to cancel noise (which is modelled as an auto regressive process or coloured noise) from the recorded event.

To achieve the above objective, pre-event data is first analysed through an adaptive filter as shown in Fig. 1. The output of this filter, $b(n)$, will be white noise if the length of the adaptive FIR predictive filter $H(z)$ is adequate. The output $c(n)$ will be

estimated coloured noise. After the trigger, the adaptive filter designed prior to trigger is considered as a fixed filter. When the signal and coloured noise pass through this fixed filter, the output $b(n)$ will be a broadband signal superimposed with white noise. The frequency contents of this broad band signal will be same as that of the post trigger part of the accelerogram with a change of amplitude. However, amplitude at this stage is not important. The output $b(n)$ of this stage is used as input to the second stage adaptive FIR filter to estimate optimum noise part of the signal (coloured noise) as shown in Fig. 2. As long as the optimum noise estimator is independent of the amplitude of the broadband signal, the filter will be good for estimation of coloured noise. The composite filter for the event is shown schematically in Fig. 3.

In the adaptive filtering problem, the filter length M has to be fixed *a priori*. For the sake of convienience, the length M of both the filters $H(z)$ and $G(z)$ are chosen to be identical. At the pre-event stage the output of filter is

$$b(n) = x(n) - c(n) \tag{1}$$

which can be written as

$$b(n) = x(n) - \sum_{i=1}^{M} h(i)x(n-i) \tag{2}$$

where $h(i)$, $i \in [1, M]$ are the filter coefficients and $c(n)$ is the coloured noise part estimated by the filter $H(z)$. Equation 2 can be written as

$$B(z) = H'(z)X(z) \tag{3}$$

where $B(z)$ and $X(z)$ are the z-transform of $b(n)$ and $x(n)$ respectively and

$$H'(z) = 1.0 - H(z)z^{-1} \tag{4}$$

$$z^{-1}H(z) = \sum_{i=1}^{M} h(i)z^{-i} \tag{5}$$

After the event, output $b(n)$ of the first stage fixed filter is the input to the second stage adaptive filter. The output of the second stage can be written as

$$y(n) = x(n) - a(n) \tag{6}$$

where

$$a(n) = \sum_{i=0}^{M-1} g(i)b(n-i) \tag{7}$$

Equation 7 can be written in z-transform as

$$A(z) = G(z)B(z) \tag{8}$$

and

$$G(z) = \sum_{i=0}^{M-1} g(i)z^{-i} \tag{9}$$

The z-transform of Eq. 6 is

$$Y(z) = X(z) - A(z) \tag{10}$$

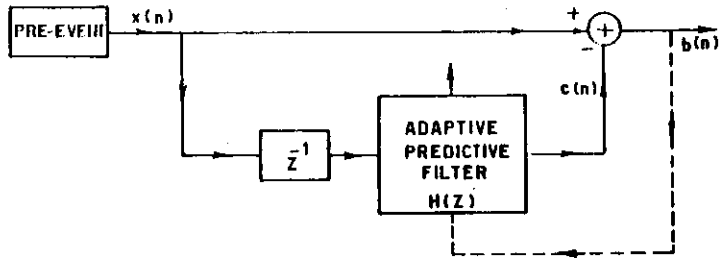

Figure 1: Adaptive filter for pre event part of the record.

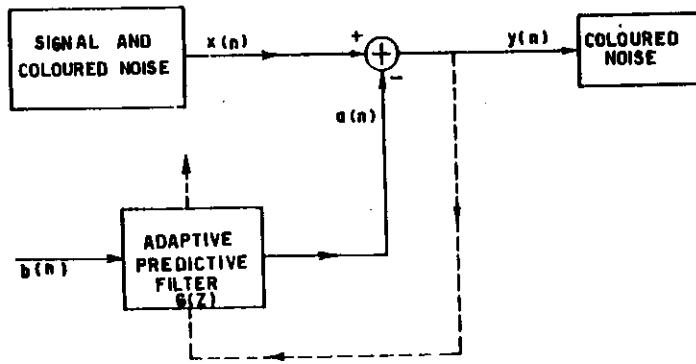

Figure 2: Second stage adaptive filter to estimate optimum coloured noise.

Using Eqs 3 and 8, it can be shown that

$$A(z) = G(z)H'(z)X(z) = F(z)X(z) \tag{11}$$

where the overall transfer function is given by

$$F(z) = \frac{A(z)}{X(z)} = G(z)H'(z) \tag{12}$$

and

$$Y(z) = \{1.0 - F(z)\}X(z) \tag{13}$$

The schemes described above are realised adaptivily and the details are given in the Appendix.

ILLUSTRATIVE EXAMPLE

Record of a digital accelerograph (Kumar et. al 1990) obtained through a shake table test is used to demonstrate the scheme presented above. Figure 4 gives the unprocessed time history of the record.

Model of Noise

The record is first analysed to identify the possible model parameters. On studying the pre-event part of the record of the digital accelerograph carefully, it can be found that the first 474 samples (at 100 SPS) is noise. The estimated mean of this sequence of 474 samples is $\bar{x} = 0.1811$ *gals*. This mean is subtracted from the data for further analysis. The choice of parameter M is an important criteria in model selection. The choice is dependent on the length of data and a measure of how close the data fits the model. The measure is the mean squared prediction error $\hat{E}_M$ of the M^{th} order prediction error filter. As M increases, $\hat{E}_M$ decreases and number of representative error samples decreases too. Moreover, for short data records spurious features get introduced. This is known as *bias versus variance dilemma*. Some of the criteria for the selection of M are based on final prediction error can be given formally as

$$\min_M \left[(K + M + 1)\hat{E}_M/(K - M - 1)\right] \tag{14}$$

$$\min_M \left[\ln(\hat{E}_M) + 2M/K\right] \tag{15}$$

$$\min_M \left[(\sum_{j=1}^{M} 1/\hat{E}_j)/K - 1/\hat{E}_M\right] \tag{16}$$

due to Akaike (1970,1974), and Parzen (1974) respectively. The plots of $M \in [0, 32]$ are shown in Fig. 5. All of them show a decreasing trend with increasing M. From this figure M is selected as 15 as there is little reduction in the ordinate of all the three

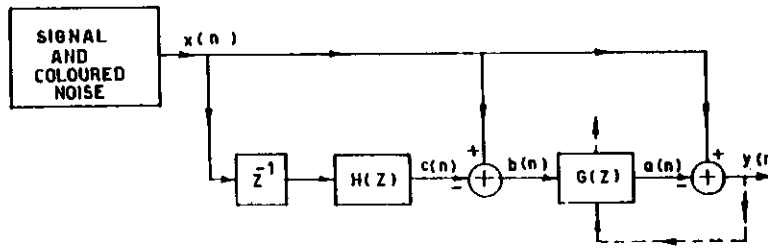

Figure 3: The composite filter for the event.

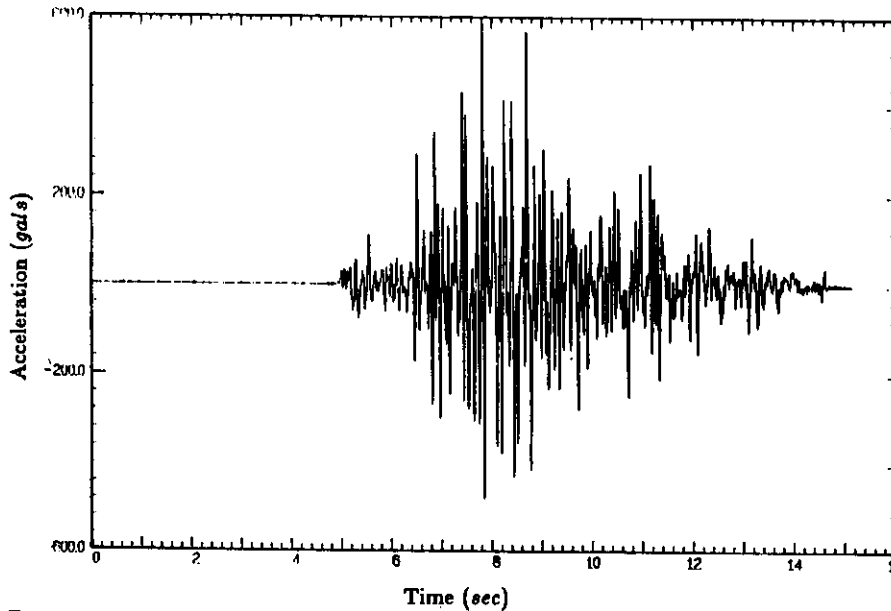

Figure 4: Recorded accelerogram (uncorrected) of horizontal motion of the shake table (channel 3).

curves of Fig. 5 beyond order 15. The data is again analysed with $M = 15$ and power spectrum given by the following equation is estimated.

$$\hat{s}(\omega) = \frac{\hat{\beta}}{\left|\hat{A}(e^{j\omega})\right|^2} \tag{17}$$

where

$$\hat{\beta} = \frac{\hat{\epsilon}_{M-1}}{2(K-M)} \tag{18}$$

and

$$\hat{\epsilon}_{M-1} = \sum_{n=M}^{K-1} \left[u^2_{M-1}(n) + v^2_{M-1}(n-1)\right] \tag{19}$$

Direct estimate of power spectrum is also made. This is carried out by modifying the data $x(n)$ by a cosine taper window weighting function (Bingham et. al, 1967)

$$d(k) = \begin{cases} 1.0 & 0 \le |k| \le \alpha K/2 \\ 0.5\left[1.0 + \cos\left\{\pi \frac{k - \alpha(K/2)}{2(1-\alpha)(K/2)}\right\}\right] & \alpha K/2 \le |k| \le K/2 \end{cases} \tag{20}$$

where α is a window parameter. A value of $\alpha = 0.8$ is used in this analysis. The autocorrelation is estimated as

$$\hat{R}(k) = \frac{1}{K-k} \sum_{i=1}^{K-k} \{x(k+i)d(k+i-\frac{K}{2})\}\{x(i)d(i-\frac{K}{2})\} \tag{21}$$

for lag $k \in [0, 256]$. The double sided z-transform of the estimated autocorrelation gives the periodogram estimate. The cosine tapered data is also used to estimate power spectrum directly by using FFT in two ways. First, the autocorrelation is estimated for 16 lags using FFT which are modified by Hamming window to reduce the effect of truncation of autocorrelation and then FFT is used to estimate power spectra (modified periodogram method). The second way to estimate power spectra of the cosine tapered data is through Welch's method in which the modified periodogram with Hamming window is estimated with 50% overlap of data. These methods are well described in Rabiner and Gold (1988). Figure 6 shows the power spectral estimate of the model (Eq. 17), periodogram, using modified periodogram method and using Welch's method. The figure shows that the average trend of the data matches quite well. The validation of the model was carried out by correlation analysis of estimated error given by

$$\hat{w}(n) = x(n) - \hat{x}(n|n-1) \tag{22}$$

and cross correlation analysis of pre-event $x(n)$ and estimated error $\hat{w}(n)$ (Ljung 1978). Figure 7 shows autocorrelation of error with 95% confidence for white noise test. For a valid model, the autocorrelation except at zero lag should be within this limit. Figure 8 shows cross correlation of pre-event with error with 95% confidence band. This figure tests the independece between pre-event and error. However, Figure 8 shows that some cross correlation exists both in the negative and positive lags. This shows that error and pre-event are not independent. However, the variation shown is not very significant and the pre-event can be reasonably modelled as coloured noise (AR process).

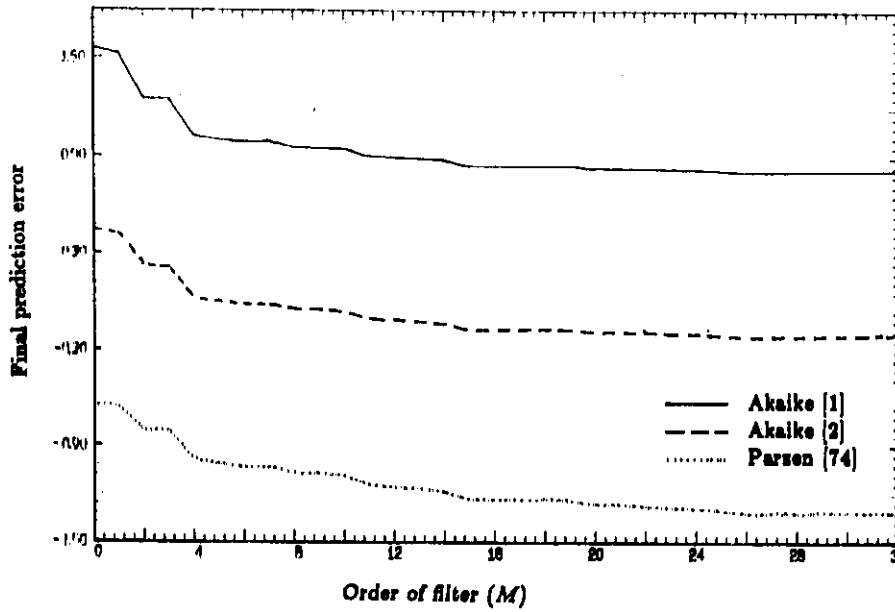

Figure 5: Final prediction error for selection of order of filter.

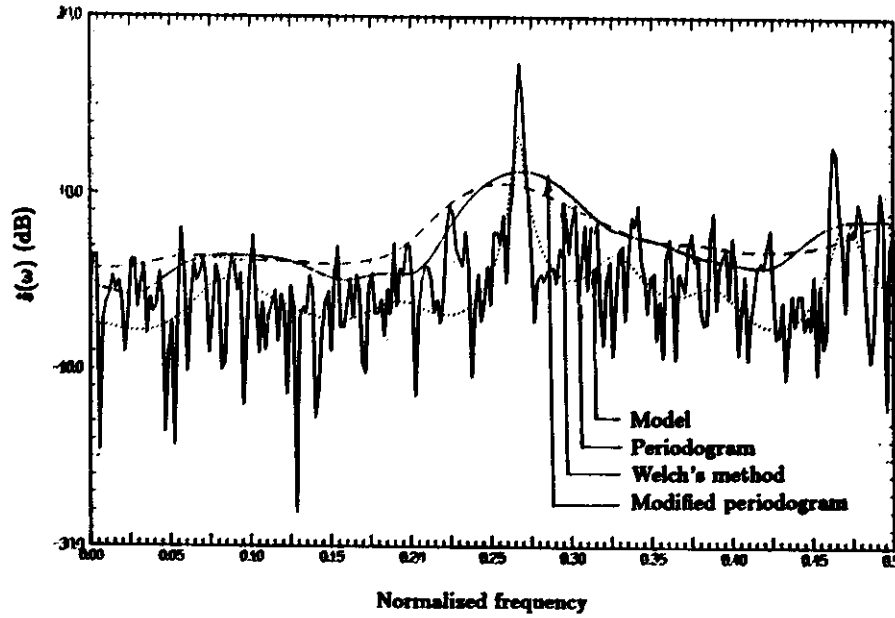

Figure 6: Comparison of power spectra of model with power spectral estimate of periodogram modified periodogram method and Welch's method.

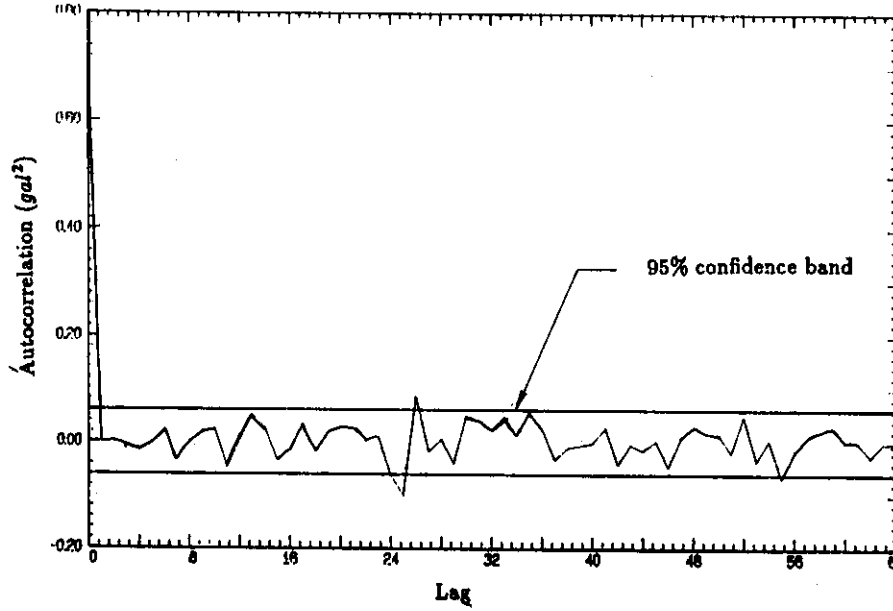

Figure 7: Autocorrelation of error with 95% confidence band for white noise test.

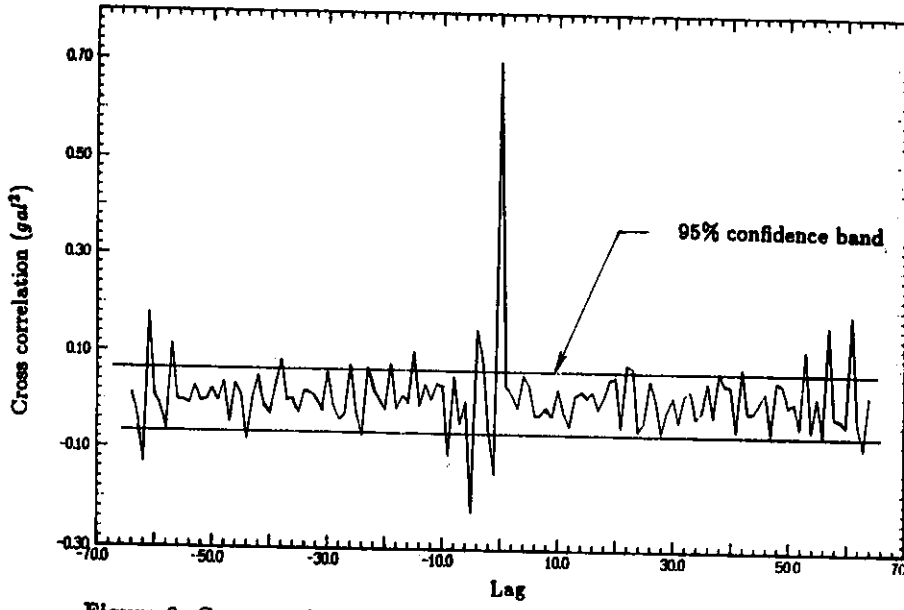

Figure 8: Cross correlation between signal and error with 95% confidence band.

Noise cancellation using adaptive algorithm

Figure 4 gives recorded accelerogram of Channel 3 (horizontal motion) of the digital accelerograph obtained from a shake table test. The data is composed of 1525 samples out of which 501 samples are of pre-event and 1024 samples are post trigger. The pre-event part of the data is the reference noise which is proposed to be used to correct the event part as per scheme outlined in the previous section. Figure 9 and Fig. 10 show the Fourier magnitude plot of pre-event and the event part respectively. From Fig 9 (for the pre-event) it can be seen that noise has peak around 27 Hz and 47 Hz. This noise is also reflected in the Fourier magnitude plot of the event in Fig. 10. The recorded data is analysed with a filter length of 16. The corresponding filter coefficients are given in Table 1 at the trigger, at the 513^{th} sample (mid-point) of the event and at the end of the event.

Table 1: Filter Coefficients of Channel 3

Index (i)	h(i) at trigger	g(i) at mid event	g(i) at end of event
1	-0.48058	0.84939	0.86304
2	-0.10905	-0.29713	-0.31795
3	-0.04464	-0.05998	-0.05198
4	0.22158	0.04907	0.04988
5	0.15222	0.06247	0.07810
6	0.22058	0.03756	0.01053
7	0.06202	0.09285	0.11163
8	0.19377	-0.10942	-0.12155
9	-0.06577	0.15652	0.17460
10	-0.08661	-0.18112	-0.20817
11	0.24126	0.03561	0.06015
12	0.09002	0.16850	0.15308
13	0.11050	0.02510	0.04858
14	0.04257	-0.06369	-0.10032
15	0.37203	0.06596	0.09439
16	0.04325	0.09378	0.08568

Figure 11 shows the magnitude plot of the adaptive filter at the trigger, at the mid point of the event and at the end of the event. This plot is between gain of the filter and normalized frequency defined as frequency divided by the sampling rate (100 SPS in this case). In this figure magnitude of $H'(z)$ of Eq. 4 is plotted at the trigger and magnitude of $F(z)$ is plotted for mid event and at the end of event. It can be seen from Fig. 11 that the gain of the adaptive filter is almost unity at most of the frequencies and it removes the coloured noise corruption of around 27 and 47 Hz from the accelerogram. Figure 12 shows the accelerogram after the adaptive filtering for Channel 3. Figure 13 show the Fourier magnitude plot of the event part of the processed accelerogram. A comparison of Figs. 10 and 13 clearly indicates that coloured noise peaks at around 27 and 47 Hz are removed in the processed record. Table 2 gives comparison of uncorrected accelerogram, corrected accelerogram and noise in frequency domain in 16 different

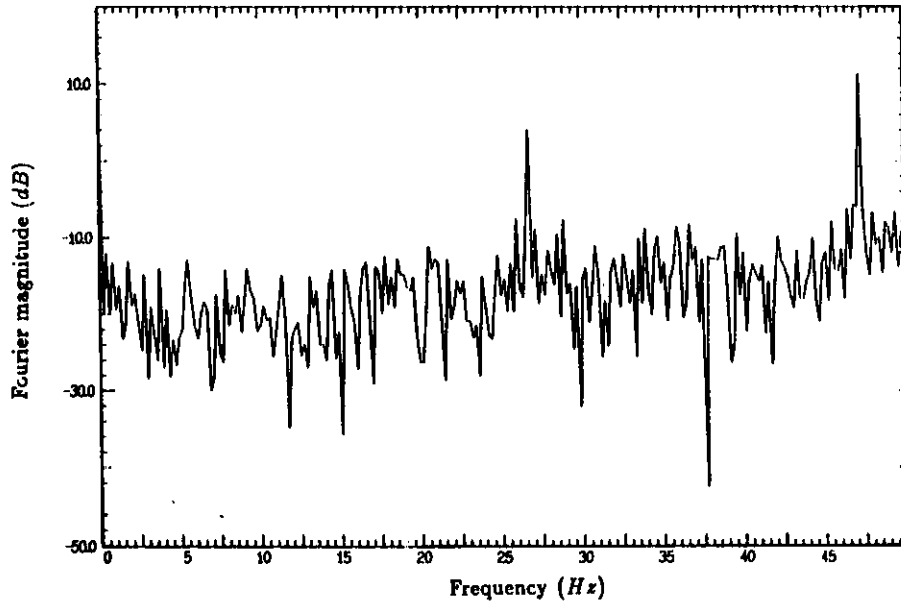

Figure 9: Fourier magnitude of pre event of uncorrected accelerogram of channel 3.

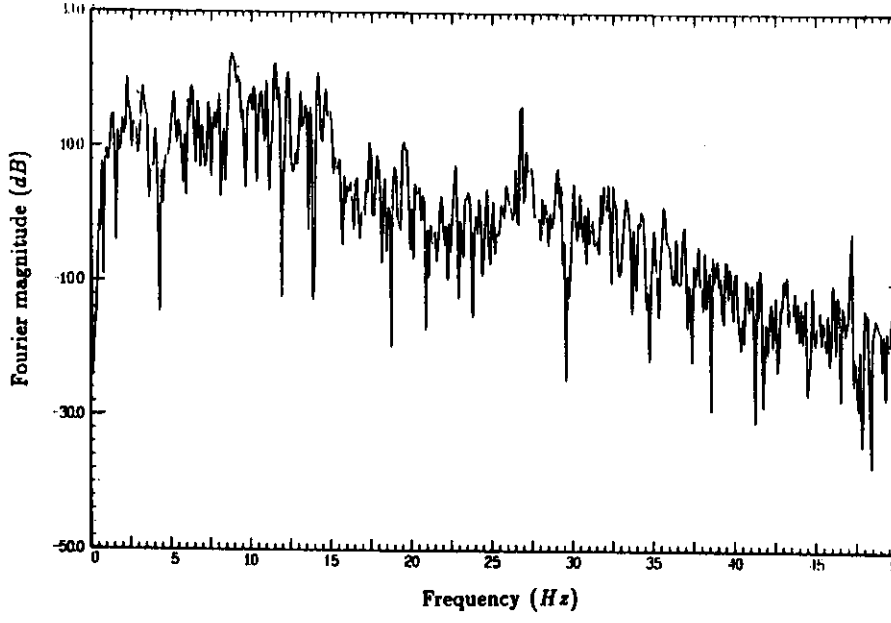

Figure 10: Fourier magnitude of event part of uncorrected accelerogram of channel 3.

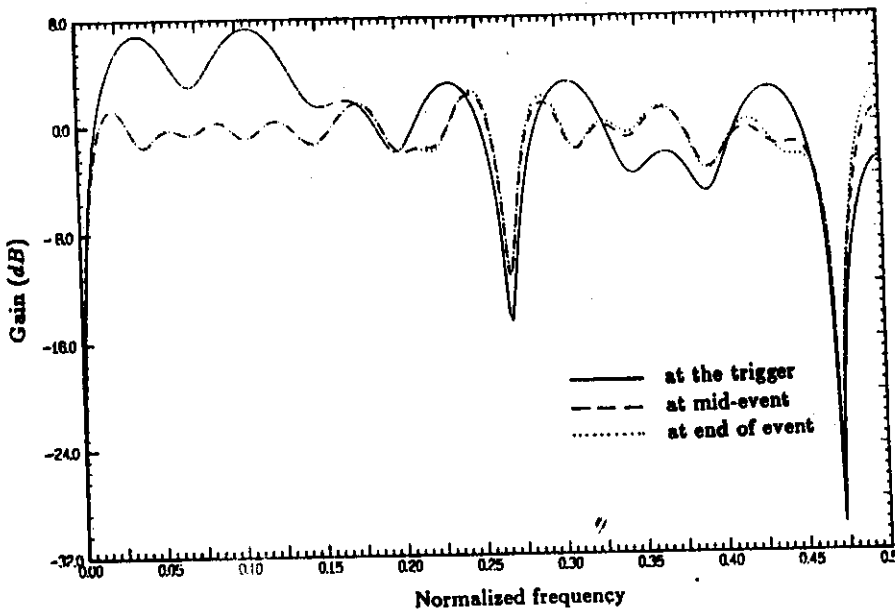

Figure 11: Magnitude of transfer function of adaptive filter of channel 3 at the trigger, at mid of event and at the end of event.

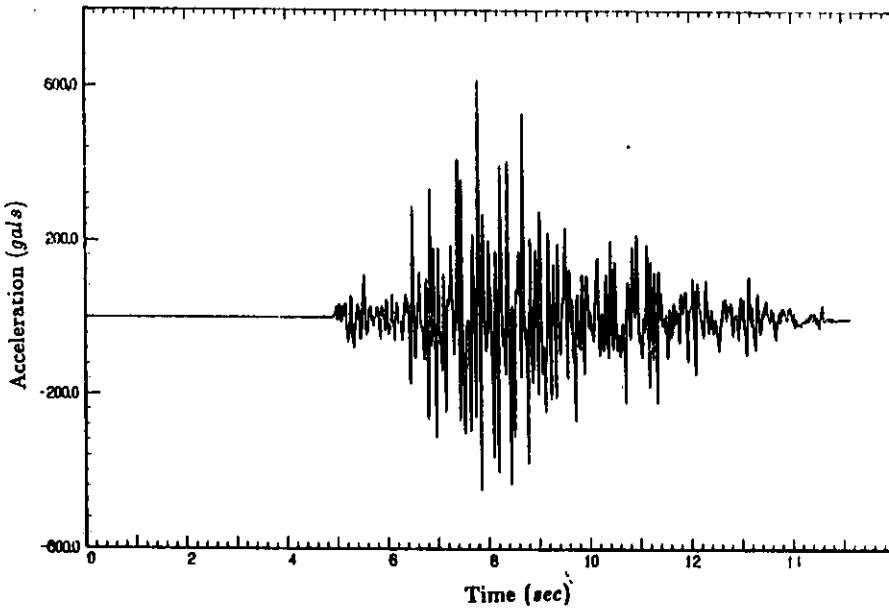

Figure 12: Accelerogram obtained after noise cancellation through adaptive filter for channel 3.

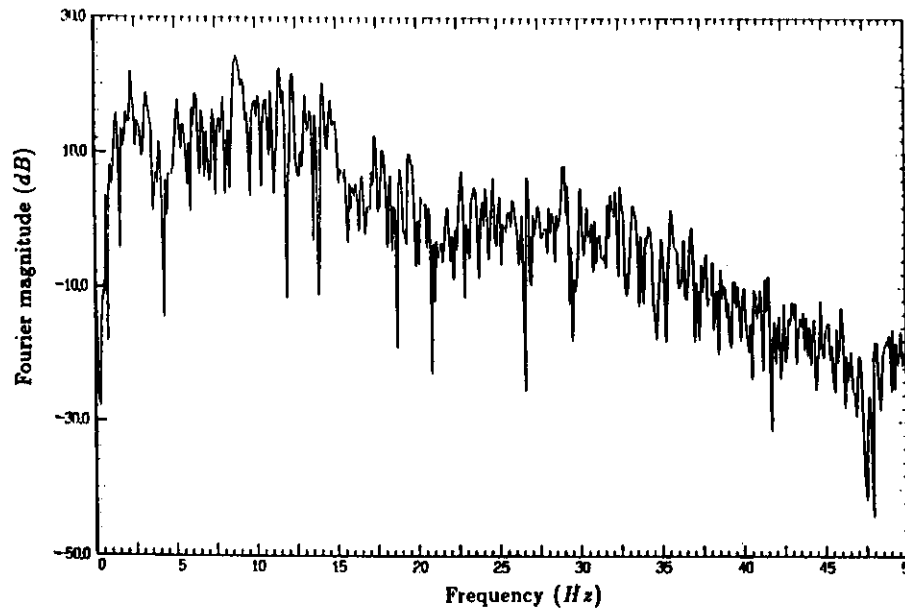

Figure 13: Fourier magnitude of event part of accelerogram obtained after noise cancellation through adaptive filter for channel 3.

frequency segments. From this table it can be seen that in the frequency ranges 26 to 29 Hz and 44 to 50 Hz, mean Fourier magnitude of the corrected accelerogram is substantially smaller than that of uncorrected accelerogram. This is due to the fact that noise in the record was predominantly of about 27 and 47 Hz (Fig. 9) which is removed by the adaptive filter.

Table 2: Comparison of Correction in Frequency Domain for Channel 3

Frequency Segment		Mean			Coefficient of Variation		
Begin (Hz)	End (Hz)	Noise (dB)	Uncorr. (dB)	Corr. (dB)	Noise	Uncorr.	Corr.
0.000	3.125	2.226	10.298	10.653	0.801	0.710	0.828
3.223	6.348	-6.510	12.027	11.510	0.507	0.609	0.632
6.445	9.570	-8.106	15.548	15.622	0.437	0.644	0.676
9.668	12.793	-7.675	15.219	15.043	0.639	0.603	0.610
12.891	16.016	-6.940	12.395	11.849	0.663	0.664	0.647
16.113	19.238	-9.043	3.182	4.306	0.608	0.515	0.540
19.336	22.461	-11.800	1.376	0.125	1.068	0.743	0.737
22.559	25.684	-10.080	-0.506	0.824	0.629	0.494	0.451
25.781	28.906	-0.021	4.136	-0.668	1.070	0.851	0.473
29.004	32.129	-16.345	-0.536	-0.999	0.596	0.561	0.661
0.000	32.910	-6.032	9.198	8.913	1.209	0.996	1.039
32.227	35.059	-19.120	-2.663	-3.261	0.524	0.606	0.637
35.156	37.988	-22.105	-6.853	-6.834	0.662	0.535	0.561
38.086	40.918	-20.931	-10.854	-12.487	0.546	0.455	0.435
41.016	43.848	-22.109	-14.160	-15.296	0.404	0.487	0.489
43.945	46.777	-19.275	-15.926	-18.633	0.582	0.456	0.462
46.875	49.707	-19.784	-16.715	-22.285	1.314	0.984	0.568
33.008	50.00	-20.442	-10.555	-11.789	0.777	0.854	0.950
0.000	50.000	-8.840	6.025	5.694	1.460	1.318	1.373

Similar results are obtained for Channel 1 of the recorded motion. Figure 14 gives recorded accelerogram of Channel 1 (vertical motion). Figure 15 and Fig. 16 show the Fourier magintude plot of pre-event and the event part respectively. From Fig 15 (for the pre-event) it can be seen that noise has peaks around 27 Hz and 47 Hz as in the case of horizontal motion. This noise is also reflected in the Fourier magnitude plot of the event in Fig. 16. The recorded data is analysed by the developed scheme described earlier with a filter length of 16. The corresponding filter co-efficients are given in Table 3 at the trigger, at the 513^{th} sample (mid-point) of the event and at the end of the event.

Figure 17 shows the magnitude plot of the adaptive filter at the trigger, at the mid point of the event and at the end of the event. Figure 18 shows the accelerogram after adaptive filtering for Channel 1. Figure 19 show the Fourier magnitude plot of the event part of the processed accelerogram. A comparison between Figs. 16 and 19 indicates that coloured noise peaks at around 27 and 47 Hz are removed in the processed

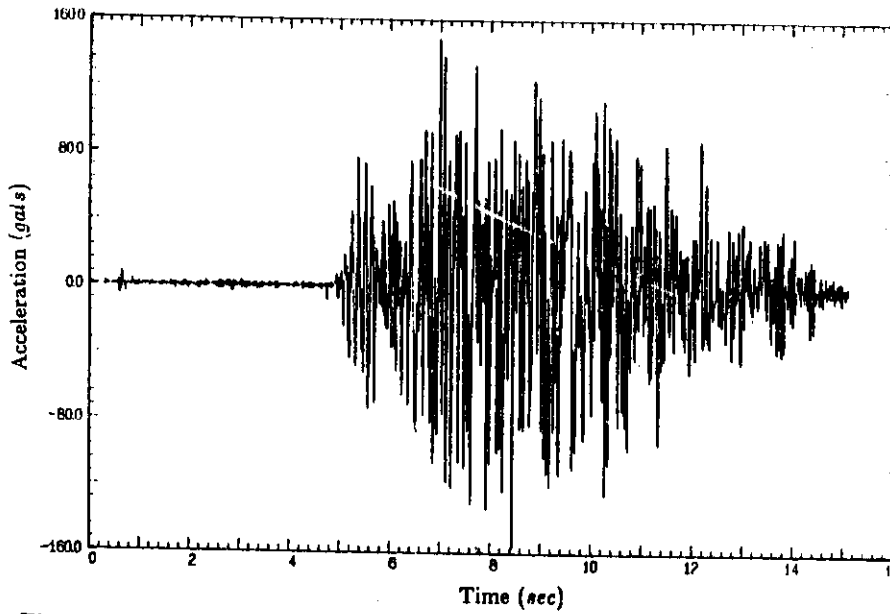

Figure 14: Recorded accelerogram (uncorrected) of horizontal motion of the shake table (channel 1).

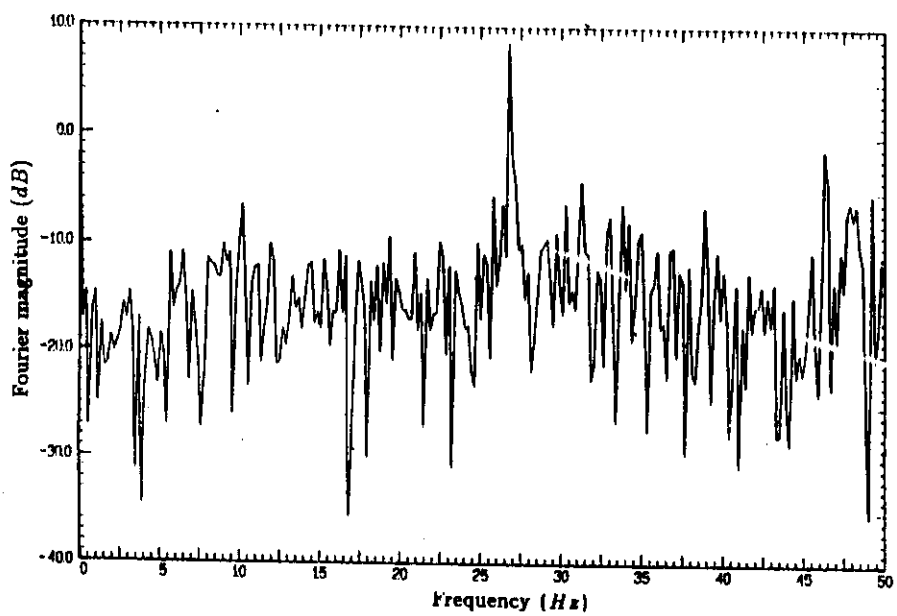

Figure 15: Fourier magnitude of pre event of uncorrected accelerogram of channel 1.

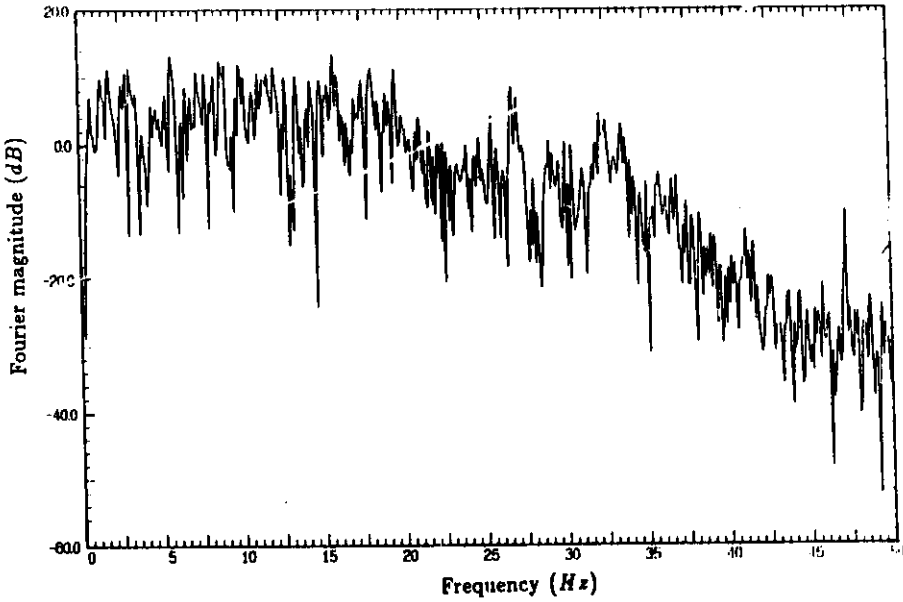

Figure 16: Fourier magnitude of event part of uncorrected accelerogram of channel 1.

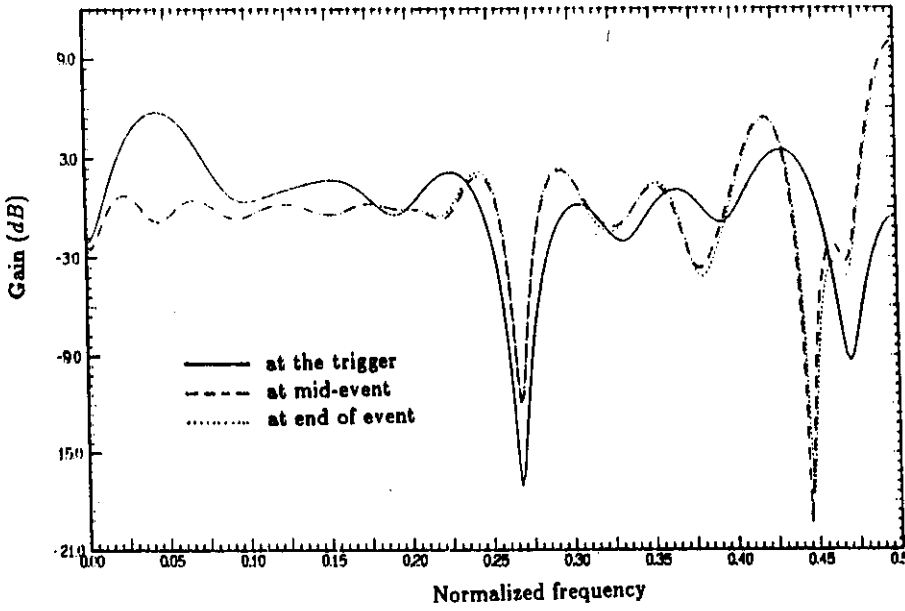

Figure 17: Magnitude of transfer function of adaptive filter of channel 1 at the trigger, at mid of event and at the end of event.

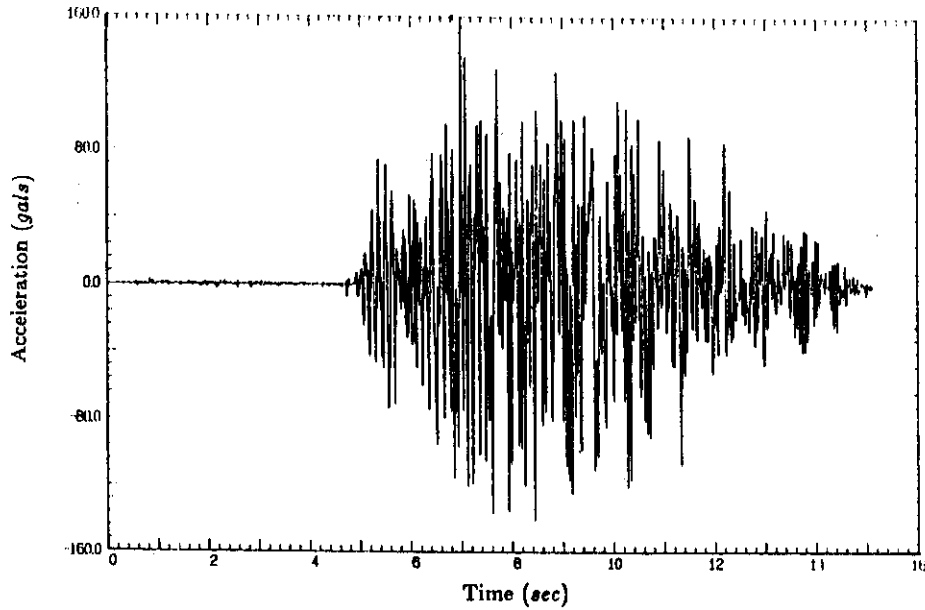

Figure 18: Accelerogram obtained after noise cancellation through adaptive filter for channel 1.

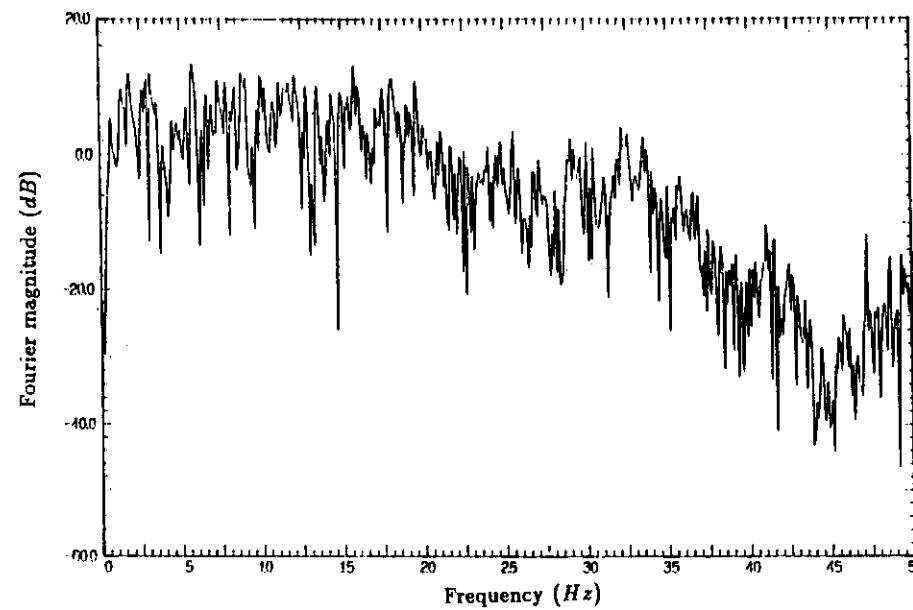

Figure 19: Fourier magnitude of event part of accelerogram obtained after noise cancellation through adaptive filter for channel 1.

Table 3: Filter Coefficients of Channel 1

Index (i)	h(i) at trigger	g(i) at mid event	g(i) at end of event
1	-0.22407	0.96726	0.97295
2	-0.19393	-0.22226	-0.22714
3	-0.07094	-0.09914	-0.10197
4	0.14804	-0.04371	-0.04566
5	-0.15908	0.18039	0.18561
6	0.01193	-0.24049	-0.23072
7	0.05175	0.13863	0.10906
8	0.15895	-0.04890	-0.01877
9	0.01187	0.24129	0.21401
10	0.04250	-0.26006	-0.21962
11	0.22831	0.29488	0.24704
12	0.07874	-0.12248	-0.08006
13	0.05981	0.26557	0.24211
14	-0.09063	-0.28710	-0.28000
15	0.18301	0.15038	0.15245
16	-0.02389	0.01591	0.01521

record. Table 4 gives comparison of uncorrected accelerogram, corrected accelerogram and noise in frequency domain in 16 different frequency segments. Similar results as discussed for channel 3 can be seen in this table also.

CONCLUSIONS

In this work, it has been shown that noise in the record of digital accelerographs can be modelled from the pre event of the record. Adaptive filters can then be designed to cancel the noise which has been modelled. A scheme based on adaptive filters is proposed which can be used effectively in removing the noise from the record of digital accelerographs.

It is important to mention here that digital accelerographs having dynamic range more than 96 dB with transducers of dynamic range of the order of 140 dB are nowadays available. This increased capability has two advantages. Firstly the accuracy or the resolution of the recorded acceleration has increased. For a 16 bit digital accelerograph having a range of $\pm 2g$, the accelerations will be multiples of approx. $g/16000$. The second advantage of large dynamic range is the capability to record very small accelerations. The first advantage of having high accuracy is not a very important one as engineering as well seismological applications of strong motion records do not need such high accuracies. The second advantage ie. the capability to record very small accelerations in addition to strong motion is most crucial. The question is whether with the increase in the dynamic range can an accelerograph perform the functions of a micro earthquake recorder also? The answer is that it can do this work only if the

Table 4: Comparison of Correction in Frequency Domain for Channel 1

Frequency Segment		Mean			Coefficient of Variation		
Begin (Hz)	End (Hz)	Noise (dB)	Uncorr. (dB)	Corr. (dB)	Noise	Uncorr.	Corr.
0.000	3.125	-12.140	4.193	4.255	0.666	0.671	0.712
3.223	6.348	-18.853	3.722	3.519	0.733	0.646	0.674
6.445	9.570	-21.612	5.431	5.316	0.635	0.576	0.572
9.668	12.793	-21.948	6.689	6.693	0.544	0.426	0.428
12.891	16.016	-23.337	4.826	4.631	0.548	0.618	0.618
16.113	19.238	-23.017	4.488	4.571	0.554	0.485	0.488
19.336	22.461	-22.567	0.313	0.039	0.526	0.636	0.653
22.559	25.684	-15.909	-4.343	-3.554	1.085	0.514	0.475
25.781	28.906	-6.849	-3.197	-7.925	1.043	0.916	0.580
29.004	32.129	-17.787	-5.660	-4.388	0.843	0.523	0.527
0.000	32.910	-16.719	2.541	2.374	1.415	0.735	0.751
32.227	35.059	-22.816	-2.953	-3.147	0.513	0.582	0.566
35.156	37.988	-25.265	-10.858	-10.683	0.492	0.527	0.576
38.086	40.918	-28.035	-18.797	-19.688	0.498	0.535	0.498
41.016	43.848	-26.574	-22.487	-20.500	0.442	0.691	0.754
43.945	46.777	-30.490	-28.557	-32.311	0.513	0.549	0.622
46.875	49.707	-24.913	-26.180	-22.865	0.896	1.141	0.782
33.008	50.00	-26.016	-15.429	-15.217	0.670	1.327	1.272
0.000	50.000	-18.924	-0.532	-0.676	1.543	1.044	1.054

background noise and the instrument noise (which may be of the same order as that of micro earthquake signal) can be filtered on-line from the record. It is in this context that the work presented here becomes important. Although in this work the analysis for removal of noise has been done off-line but enough care has been taken to ensure that the developed scheme can be used for on-line recording using DSP chips. This is perhaps the only way that a digital accelerograph can also be used to record micro earthquakes.

REFERENCES

1. **Akaike, H. (1970)** —On a Semi Automatic Power Spectrum Estimation Procedure. *Proceedings Third Hawaii International Conference on System Science*, **Part 2**, pp974–977.

2. **Akaike, H. (1974)** —A New Look at Statistical Model Identification. *IEEE Transaction on Automatic Control*, **Vol. AC–19, December**, pp716–723.

3. **Amini, A. and Trifunac, M.D. (1983)** —Analysis of Feed Back Transducer. *Report of University of Southern California, Report no. 83–03.*

4. **Amini, A. and Trifunac, M.D. (1985)** —Analysis of Force Balance Accelerometer. *Soil Dynamics and Earthquake Engineering*, **Vol.4, No.2**, pp.82–90.

5. **Bingham, C., Godfrey, M.D. and Tukey, J.W. (1967)** —Modern Technique of Power Spectrum Estimation. *IEEE Transaction on Audio and Electroaccoustics*, **Vol. AU–15, No.2**, pp56–66.

6. **Goodwin, G.C. and Sin, K.S. (1984)** —Adaptive Filtering Prediction and Control. *Prentice Hall, Inc., Englewood Cliffs, N.J.*.

7. **Householder, A.S. (1964)** —The Theory of Matrices and Numerical Analysis. *Blaisdell, Waltham, Mass.*.

8. **Iwan, W.D., Moser, M.A. and Peng, C.Y. (1985)** —Some Observations on Strong Motion Earthquake Measurement Using a Digital Accelerograph. *Bulletin of Seismological Society of America*, **Vol.75, No. 5**, pp.1225–1246.

9. **Kumar, A. (1993)** —New Schemes for Processing Accelerograms. *Ph.D. Thesis, Department of Earthquake Engineering, University of Roorkee, Roorkee, India.*

10. **Kumar, A., Gupta, N.C., Basu, S., Panday, A.D., Bansal, M.K. and Verma, V.K. (1990)** —Microprocessor Based Strong Motion Accelerograph. *Proceedings Ninth Symposium on Earthquake Engineering, University of Roorkee, Roorkee*, **Vol. 1.**

11. **Lee, V.W. (1984)** —Recent Developments in Data Processings of Strong Motion Accelerograms. *Proceedings Eighth World Conference on Earthquake Engineering, San Francisco, USA*, **Vol. II**, pp.119–126.

12. **Ljung, L. (1978)** —System Identification Theory for the Users. *Prentice Hall Inc., Englewood, Calif., N.J.*

13. **Parzen, E. (1974)** —Some Recent Advances in Time Series Modelling. *IEEE Transaction on Automatic Control*, **Vol. AC–19, December**, pp724–730.

14. **Rabiner, L.R. and Gold, B. (1988)** —Theory and Application of Digital Signal Processing. *Prentice Hall of India Private Ltd., New Delhi.*

APPENDIX

Adaptive algorithm

The FIR filter described in the paper can be designed adaptivily through recursive least square (RLS) algorithm (Goodwin and Sin 1984; Ljung 1978). Since the noise can be reasonably represented as an AR process, the noise removal can be tried as direct form recursive filter. The algorithm can be conveniently described in matrix notation. A time index is used to denote recursion in time. Let at instant n, $\Theta_M(n)$ be the filter coefficient vector given as

$$\Theta_M(n) = \begin{Bmatrix} \theta(0,n) \\ \theta(1,n) \\ \theta(2,n) \\ \vdots \\ \theta(M-1,n) \end{Bmatrix} \tag{23}$$

Similarily the input vector to the filter is

$$\mathbf{X}_M(n) = \begin{Bmatrix} x(n) \\ x(n-1) \\ \vdots \\ x(n+1-M) \end{Bmatrix} \tag{24}$$

Let $y(n)$ be the desired output of the filter which is observed for a duration of N samples. The coefficient vector $\theta_M(n)$ is determined by minimizing a weighted sum of magnitude square errors

$$\varepsilon = \min \left[\sum_{n=1}^{N} \prod_{k=n+1}^{N} \lambda(k) e^2(n) \right] \tag{25}$$

where estimation error is

$$e(n) = y(n) - \hat{y}(n) = y(n) - \mathbf{X}_M^T(n)\, \Theta_M(n) \tag{26}$$

The superscript T denotes as transpose of matrix and $\lambda(k)$ is the time varying *forgetting factor* used to track the possible nonstationarity of the signal better and is given by

$$\lambda(k) = 1 - \lambda_0 + \lambda_0 \lambda(k-1) \tag{27}$$

By differentiating Eq. 25 with respect to the filter coefficients, the so called normal form of the equation is obtained as

$$\mathbf{R}_M(n)\,\boldsymbol{\Theta}_M(n) = \mathbf{r}_M(n) \tag{28}$$

where

$$\mathbf{R}_M(n) = \sum_{k=1}^{n} \prod_{i=k+1}^{n} \lambda(i)\mathbf{X}_M(k)\mathbf{X}_M^T(k) \tag{29}$$

and

$$\mathbf{r}_M(n) = \sum_{k=1}^{n} \prod_{i=k+1}^{n} \lambda(i)\mathbf{X}_M(k)y(k) \tag{30}$$

The solution of Eq. 28 is then

$$\boldsymbol{\Theta}_M(n) = \mathbf{R}_M^{-1}(n)\mathbf{r}_M(n) \tag{31}$$

However, in the adaptive implementation, it is impractical to solve the set of M linear equations at the arrival of each new signal component. The rank-one updating properties are used in adaptive RLS algorithm to arrive at a n^{th} stage solution from the known $(n-1)^{th}$ stage. The matrix $\mathbf{R}_M(n)$ and vector $\mathbf{r}_M(n)$ satisfy

$$\mathbf{R}_M(n) = \lambda(n)\mathbf{R}_M(n-1) + \mathbf{X}_M(n)\mathbf{X}_M^T(n) \tag{32}$$

and

$$\mathbf{r}_M(n) = \lambda(n)\mathbf{r}_M(n-1) + \mathbf{X}_M(n)y(n) \tag{33}$$

Since inverse of $\mathbf{R}_M(n)$ is needed for solution of Eq. 31, the algorithm only stores the same. Denoting

$$\mathbf{R}_M^{-1}(n) = \mathbf{P}_M(n) \tag{34}$$

and using matrix inversion lemma (Householder 1964), the recursive computational form can be obtained as

$$\mathbf{P}_M(n) = \lambda^{-1}(n)\left[\mathbf{P}_M(n-1) - \frac{\mathbf{P}_M(n-1)\mathbf{X}_M(n)\mathbf{X}_M^T(n)\mathbf{P}_M(n-1)}{\lambda(n) + \mathbf{X}_M^T(n)\mathbf{P}_M(n-1)\mathbf{X}_M(n)}\right] \tag{35}$$

For computational convenience, *a priori* estimate of $\hat{y}(n|n-1)$, estimation error $e(n|n-1)$ and Kalman gain factor $\mathbf{K}_M(n|n-1)$ are denoted as

$$\hat{y}(n|n-1) = \mathbf{X}_M^T(n)\,\boldsymbol{\Theta}_M(n-1) \tag{36}$$

$$e(n|n-1) = y(n) - \hat{y}(n|n-1) \tag{37}$$

$$\mathbf{K}_M(n|n-1) = \lambda^{-1}(n)\mathbf{P}_M(n-1)\mathbf{X}_M(n) \tag{38}$$

Thus, it can be seen that *a priori* solution is the solution of the problem at instant $n-1$. A scalar $\mu(n)$ is defined as

$$\mu(n) = \mathbf{K}_M^T(n|n-1)\mathbf{X}_M(n) \tag{39}$$

or

$$\mu(n) = \lambda^{-1}(n)\mathbf{X}_M^T(n)\mathbf{P}_M(n-1)\mathbf{X}_M(n) \tag{40}$$

The *posterior* Kalman gain vector $\mathbf{K}_M(n)$ can be given as

$$\mathbf{K}_M(n) = \frac{1}{1+\mu(n)}\mathbf{K}_M(n|n-1) = \mathbf{P}_M(n)\mathbf{X}_M(n) \tag{41}$$

Thus Eq. 35 can be written as

$$\mathbf{P}_M(n) = \lambda^{-1}(n)\mathbf{P}_M(n-1) - \mathbf{K}_M(n)\mathbf{K}_M^T(n|n-1) \tag{42}$$

The filter coefficients of Eq. 31 with the use of rank one updating property, Eqs. 32 and 33 reduces to

$$\boldsymbol{\Theta}_M(n) = \boldsymbol{\Theta}_M(n-1) + \mathbf{P}_M(n)\mathbf{X}_M(n)\left[y(n) - \mathbf{X}_M^T(n)\,\boldsymbol{\Theta}_M(n-1)\right] \tag{43}$$

Use of Eqs 36, 37 and 41 give

$$\boldsymbol{\Theta}_M(n) = \boldsymbol{\Theta}_M(n-1) + \mathbf{K}_M(n)e(n|n-1) \tag{44}$$

Using Eqs. 37, 40, 41 and 44, the *posterior* estimation error $e(n)$ and estimate $\hat{y}(n)$ can be obtained as

$$e(n) = \frac{1}{1+\mu(n)}e(n|n-1) \tag{45}$$

and

$$\hat{y}(n) = \mathbf{X}_M^T(n)\,\boldsymbol{\Theta}_M(n) = y(n) - e(n) \tag{46}$$

It should be noted that *posterior* solution is the solution of the filtering problem at stage n.

To start the recursion, $\mathbf{P}_M(0)$ will be needed which will be high and is generally taken as

$$\mathbf{P}_M(0) = \frac{\mathbf{I}_M}{\delta} \tag{47}$$

where $\mathbf{I}_M$ is an identity matrix. However, the algorithm is insensitive to the value of δ and commonly used value is $\delta = 0.01$. The λ_0 defined in Eq. 27 is customarily taken as $\lambda_0 = 0.99$ and $\lambda(0) = 0.95$. The computation steps of adaptive RLS can be summarized as follows:

1. Initialize $\boldsymbol{\Theta}_M(0) = \boldsymbol{\Theta}_M$ where $\boldsymbol{\Theta}_M$ is assumed as the starting value and $y(n) = x(n) = 0.0$ for $n \leq 0$.

   For $n \in [1, N]$ the steps will be the following

2. Compute forgetting factor as

$$\lambda(n) = 1 - \lambda_0 + \lambda_0\lambda(n-1) \tag{48}$$

3. Compute *a priori* Kalman gain as

$$\mathbf{K}_M(n|n-1) = \lambda^{-1}(n)\mathbf{P}_M(n-1)\mathbf{X}_M(n) \tag{49}$$

4. Compute scalar $\mu(n)$ as

$$\mu(n) = \mathbf{K}_M^T(n|n-1)\mathbf{X}_M(n) \tag{50}$$

5. Compute *posterior* Kalman gain as

$$\mathbf{K}_M(n) = \frac{1}{1+\mu(n)}\mathbf{K}_M(n|n-1) \tag{51}$$

6. Compute inverse of correlation matrix as

$$\mathbf{P}_M(n) = \lambda^{-1}(n)\mathbf{P}_M(n-1) - \mathbf{K}_M(n)\mathbf{K}_M^T(n|n-1) \tag{52}$$

7. Compute *a priori* estimate and estimation error as

$$\hat{y}(n|n-1) = \mathbf{X}_M^T(n)\,\boldsymbol{\Theta}_M(n-1) \tag{53}$$

$$e(n|n-1) = y(n) - \hat{y}(n|n-1) \tag{54}$$

8. Compute *posterior* error, estimate and update of filter coefficients

$$e(n) = \frac{1}{1+\mu(n)}e(n|n-1) \tag{55}$$

$$\hat{y}(n) = y(n) - e(n) \tag{56}$$

$$\boldsymbol{\Theta}_M(n) = \boldsymbol{\Theta}_M(n-1) + \mathbf{K}_M(n)e(n|n-1) \tag{57}$$

In the analysis of the data by the scheme δ was taken as 0.01 and the parameter λ_0 and $\lambda(0)$ were taken as 0.99 and 0.95 respectively.